JOURNAL OF PROPULSION AND POWER
Vol. 22, No. 3, May–June 2006

Momentum and Heat Flux Measurements Using an Impact Target in Flowing Plasma

D. Gregory Chavers*
NASA Marshall Space Flight Center, Huntsville, Alabama 35812
Franklin R. Chang-Díaz†
NASA Johnson Space Center, Houston, Texas 77058
Claude Irvine‡
NASA Marshall Space Flight Center, Huntsville, Alabama 35812
and
Jared P. Squire§
Muniz Engineering, Houston, Texas 77058

An impact target plate was used to determine the momentum and heat flux quantities from a helicon plasma source. The plasma source is the first stage of the Variable Specific Impulse Magnetoplasma Rocket, which uses radio frequency waves to create and energize a flowing plasma. The momentum and heat flux quantities are determined separately and agree favorably. They also agree with expected flux quantities calculated from the plasma parameters determined by other probes. The momentum and heat flux quantities were obtained at two axial locations in the exhaust or magnetic nozzle region of the device using helium and argon propellant. Only data from the plasma source are used, which shows that the plasma source does produce a flowing plasma with significant momentum. The flux data at the two axial locations verify the increase in momentum as the plasma flows through the diverging magnetic field in the magnetic nozzle region. Although the axial location for maximum momentum (or thrust) was not determined, forces of several millinewtons were measured for a combined neutral particle and plasma flow. The ionization fraction for these data was approximately 22%. Neutral particles entrained in the flow provided a significant part of the flow momentum thereby contributing to the potential thrust. The technique of measuring the momentum flux and heat flux in a flowing plasma is described.

Nomenclature

A	=	cross-sectional area of plasma beam
A_r	=	radiating area of target
c_p	=	specific heat
c_s	=	sound speed
E_{rec}	=	energy released from plasma recombination
F	=	force on momentum flux sensor
g_0	=	acceleration due to gravity at sea level
I_{sp}	=	specific impulse
k	=	thermal conductivity of material
k_B	=	Boltzmann's constant
M	=	Mach number of ions measured by Mach probe
m_i	=	mass of ion
m_n	=	mass of neutral
$\dot{m}$	=	mass flow rate
n_e	=	electron number density
n_i	=	ion number density
n_n	=	neutral number density
P_e	=	electron pressure
P_i	=	ion pressure
q_{net}	=	net power to surface
q_{rec}	=	power due to recombination energy
$q(x, t)$	=	heat flux in material as a function of x and t
R_{iE}	=	energy reflection coefficient
r	=	radius
$S(r, t)$	=	source term in heat conduction equation
T	=	temperature
T_{ch}	=	temperature of chamber as viewed from target
T_e	=	electron temperature
T_i	=	ion temperature
T_p	=	temperature of target plate
T_s	=	temperature of heat sink
t	=	time
v_i	=	velocity of ion
v_n	=	velocity of neutral
z	=	axial distance
α	=	thermal diffusivity of material
Γ_i	=	ion number rate
Γ_n	=	neutral number rate
δ	=	heat conduction penetration depth
ε	=	emissivity of target
ε_0	=	permittivity constant
λ_D	=	Debye length
ρ	=	mass density
σ	=	Stephan–Boltzmann constant
τ	=	thermal conduction penetration time
ϕ	=	electric potential
ϕ_f	=	floating potential

Received 29 January 2004; revision received 4 April 2005; accepted for publication 25 August 2005.

*Research Scientist, Propulsion Research Center. Member AIAA.
†Astronaut, Advanced Space Propulsion Laboratory Director.
‡Research Scientist, Propulsion Research Center.
§Research Scientist, Advanced Space Propulsion Laboratory.

I. Introduction

AS plasma is ejected from a plasma thruster, the momentum and heat flux quantities may be measured, which provide useful information about the flowing plasma. The axial locations of measurement reported in this paper are in the magnetic nozzle region of the device where the plasma is accelerating and still following the external magnetic field. The flow of momentum and heat in the magnetic nozzle region is very important toward understanding the operation of the device and for optimizing the device as a plasma thruster. A properly shaped magnetic nozzle will permit the flowing

plasma to detach from the thruster, and the location of detachment is defined by Arefiev and Breizman.[1] The axial locations for the measurements in this paper are upstream of the detachment location. The momentum flux measurement at several locations also reveals information about the acceleration of the plasma and neutral particle jets. The heat flux quantity can verify information about the plasma flow, such as the frozen in flow loss, which is potential energy between the electrons and ions in the flow and is also equivalent to the ionization energy of the propellant atom. When the ion and electron recombine, energy equivalent to the ionization energy is released and is known as the recombination energy.

In this paper, flow characteristics such as ion and neutral flow velocity as verified by measurements inside the magnetic nozzle region of the device are discussed. Recent modifications to the test facility will permit measurements to be made at locations farther downstream in the magnetic nozzle region after near the detachment location and will be reported in a subsequent submission. The flux quantities were determined using a flat plate probe placed in the flowing plasma. A brief description is given of the test facility before describing the flux tests. A force from the flowing plasma and neutral particle jets on the flat plate probe will be determined from the momentum flux and will be compared to values calculated using measured plasma parameters from electrostatic probes. The plasma parameters will also be used to calculate a heat flow to the plate and will be compared to the measured values of heat flow. The plasma-surface recombination process is the mechanism for allowing recovery of the recombination energy in this experiment and involves the neutralization of the ions at the surface of the material by the Auger neutralization process (see Ref. 2).

The fast neutral particles, resulting from charge exchange collisions near the exit of the plasma source, carry a significant portion of the momentum. Allowing neutrals in the exhaust flow, either by injection of neutrals at the exit of the helicon or by designing the helicon to only partially ionize the flow, may permit increased thrust, at the expense of I_{sp}, but without significantly reducing the thruster efficiency at lower I_{sp}. This is possible because the impact cross section for ion–neutral collision is much greater than the impact cross section for electron–neutral collision for the plasma parameters in acceleration region of this experiment. Using the charge exchange collision for this purpose is only beneficial for a limited range of neutral gas densities. Acceleration of the ions by the ambipolar electric field will be discussed along with the collisional process of ion-neutral charge exchange, which provides a mechanism for ejecting fast neutrals.

II. Experimental Method (Test Facility)

The experiment was conducted at the Advanced Space Propulsion Laboratory, NASA Johnson Space Center, Houston, Texas, in the variable specific impulse magnetoplasma rocket (VASIMR) test facility, VX-10 (Ref. 3). The VASIMR thruster concept uses radio waves to ionize a gas by exciting helicon modes via a helicon antenna. The VASIMR team is also investigating the use of radio waves to heat preferentially the ions produced by the helicon plasma source to increase the ion exhaust velocity. The ion booster antenna operates in the ion cyclotron rage of frequencies. Heating of the ions will provide greater specific impulse.[4] The VASIMR test facility uses liquid nitrogen-cooled, copper-wound solenoids to generate an axisymmetric magnetic field. Plasma is generated near the axis of the magnet set, as shown in Fig. 1, from a helicon source using rf frequencies of 13.56 or 25 MHz to excite the electrons sufficiently for ionization to occur. The plasma is confined radially by the magnetic field but is allowed to flow in the axial direction. The region of interest for this investigation is the exhaust region identified in Fig. 1 and is about 20 cm downstream of the ion booster antenna.

III. Momentum Flux Measurement

A momentum flux sensor was developed to measure the momentum flux of the combined neutral and charged particle jets.[5] This sensor consists of four uniaxial strain gauges mounted on a 6AL-4V titanium beam in a Wheatstone bridge configuration. An alumina rod was used to connect the titanium beam to a flat plate

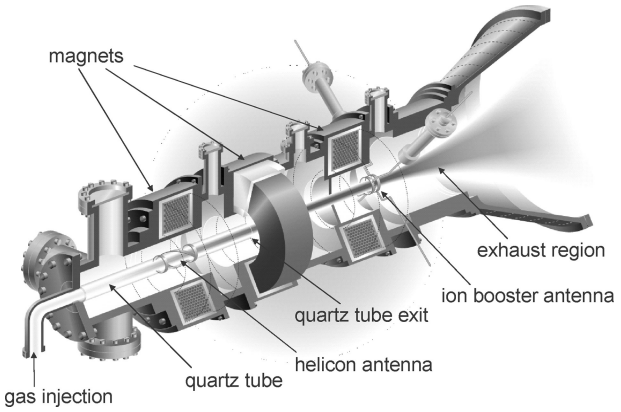

Fig. 1 VASIMR test facility primary components.

target. The target was then immersed in the plasma. The alumina rod serves to isolate the target electrically and thermally as well as provide a moment arm to amplify the strain in the titanium beam. The alumina rod also allows the strain gauges to be located outside the plasma beam and to be shielded from rf noise. Figure 2a shows a schematic of the momentum flux sensor with a 5-cm target and Fig. 2b shows a 15.2-cm-diam target immersed in the plasma. Several diameter targets have been used. Targets larger in diameter than the plasma beam were used in all of the following measurements. Through proper calibration with known forces applied to the target plate, a thrust may be inferred from the momentum flux sensor. The test configuration was not optimized to provide high thrust but was used to investigate the helicon as a plasma source. However, forces of several millinewtons were measured on the target plate.

The momentum flux measurement was used to verify the kinetic energy in the plasma flow. The momentum flux at the surface of the flat target may be calculated from the momentum equation given by

$$\frac{\mathrm{d}}{\mathrm{d}z}\left(n_i m_i v_i^2 + P_i + P_e + n_n m_n v_n^2\right) = 0 \tag{1}$$

where ionizations have been neglected in the exhaust. The last term on the left-hand side of Eq. (1) accounts for fast neutral particles resulting from charge exchange collisions near the plasma source. Charge exchange collisions are neglected downstream of the quartz tube exit because the plasma and neutral density decrease causing the mean free path for collisions to increase sufficiently in this region. At the floating plate, $P_e \approx 0$ because most of the electrons are reflected by the sheath electric field. The sheath thickness is approximately $10\lambda_D$, where the Debye length is given by

$$\lambda_D = \sqrt{\left(\varepsilon_0 k_B T_e \big/ n_e e^2\right)} \approx 2.5 \times 10^{-5}\ \mathrm{m} \tag{2}$$

From conservation of momentum flux, the change in momentum at the plate may be equated to plasma parameters just upstream of the sheath. The change in momentum is the net force on the plate given by

$$F = A\left(n_e k_B T_e + n_i m_i v_i^2 + n_n m_n v_n^2\right) \tag{3}$$

where the change in momentum from the sheath electric field is equal and opposite to the force caused by the surface charge density on the plate. Equation (3) represents the force on the plate based on the plasma parameters just outside the sheath including a term (last term on right-hand side) to account for the neutral particles. The floating sheath tends to transfer power to ions from the electrons. The triple langmuir probe was used to determine the radial density profile for the plasma terms in Eq. (3). The langmuir probe data were taken at $z = 1.55$ while the force plate at $z = 1.72$ was inserted and removed. More discussion of the force calculations will be given in Sec. VI.

Figures 3 and 4 show data for force, neutral pressure upstream of the plasma source, and injected flow rate of propellant. Figure 3 shows the relative locations of each measured quantity and the test

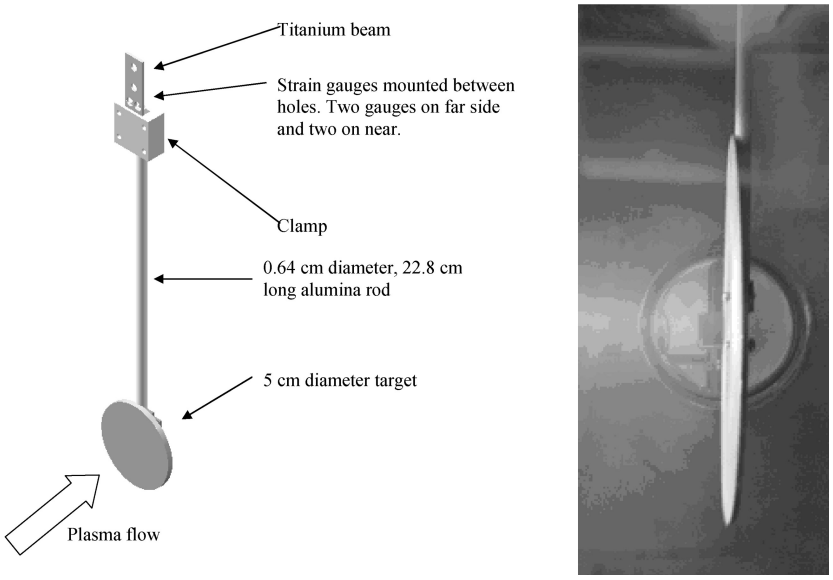

Fig. 2 Momentum flux sensor shown with two targets of different diameter: a) schematic of momentum flux sensor and b) 15.2-cm-diam target in helium plasma.

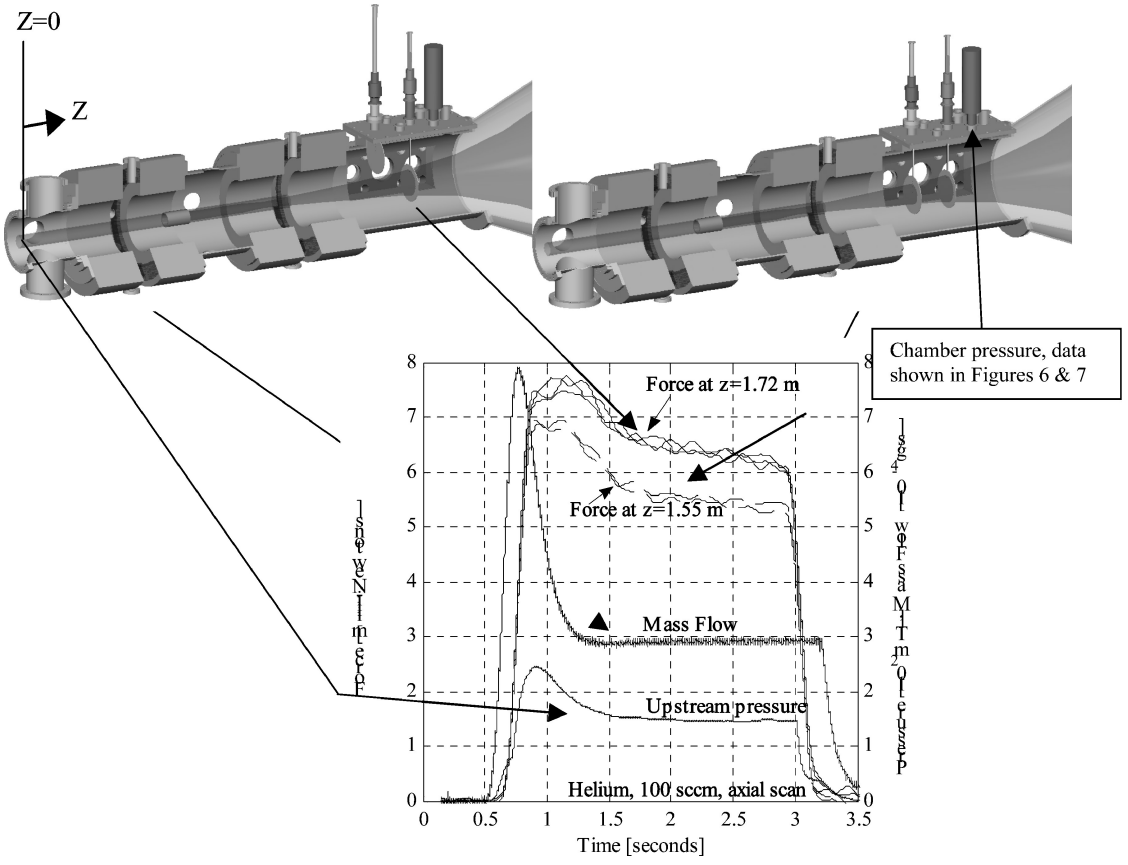

Fig. 3 Test setup and force measured at 1.55 and 1.72 m, pressure in quartz tube at $z = 0.0$ m, and gas flow into quartz tube.

setup. The plasma source is near the left ($Z \sim 0$) of each test setup, and the force sensor located farther into the exhaust region measures higher force. The higher force on the most downstream force sensor is attributed to acceleration of the ions by the ambipolar electric field and will be discussed later. Figures 5 and 6 show the neutral background pressure as measured in the vacuum chamber near the force sensors as shown in Fig. 3.

Although the mass flow rate of the argon propellant was higher than the mass flow rate of the helium, the volume flow rate was lower, 100 standard cm^3/min (SCCM) for helium and 30 SCCM for argon. Also, the thermal velocities of the argon ions and neutrals were lower than the helium ions and neutrals due to the higher mass of the argon atom. Therefore, the transient gas pressure rise in the quartz tube beneath the helicon antenna was slower for argon than for helium as represented by the upstream pressure in Figs. 3 and 4. The slower rise in pressure for the argon is also observed in the force measurements. Based on the neutral pressure, the mean free path for charge exchange is reduced from over 2 m to 0.4 m by the end of the plasma shot for helium and from almost 3 m to about 1 m for argon.[6] Because the flow rate of argon was less than that of helium, the neutral background pressure in the chamber was less when using argon.

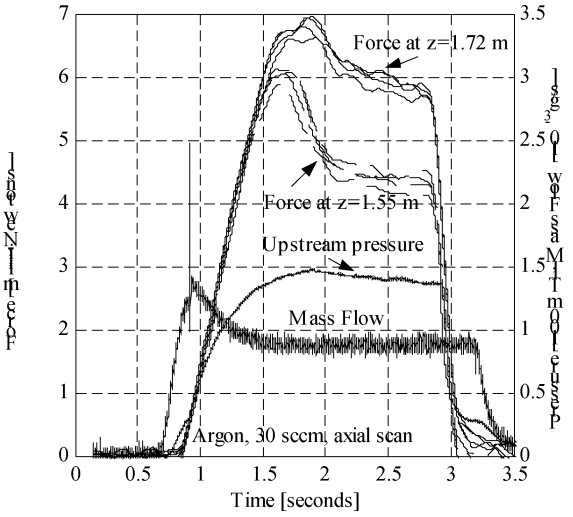

Fig. 4 Force at two locations using argon propellant at 0.89 mg/s (30 SCCM).

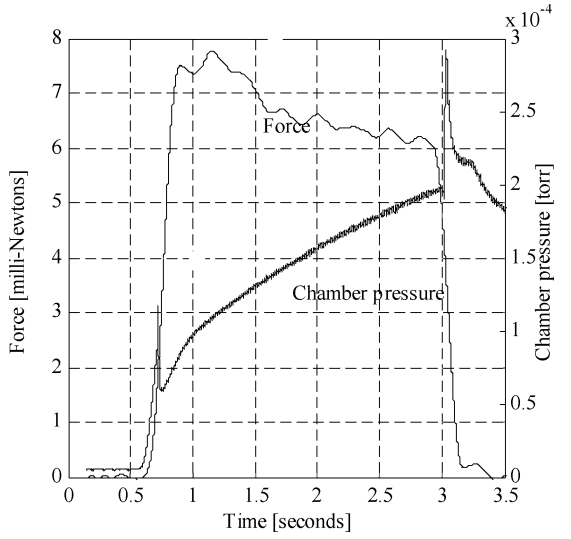

Fig. 5 Force and chamber pressure vs time using helium propellant at 0.30 mg/s (100 SCCM).

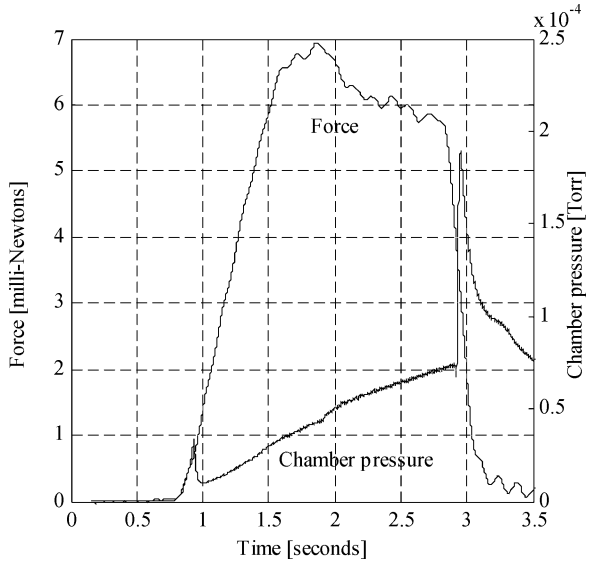

Fig. 6 Force and chamber pressure vs time using argon propellant at 0.89 mg/s (30 SCCM).

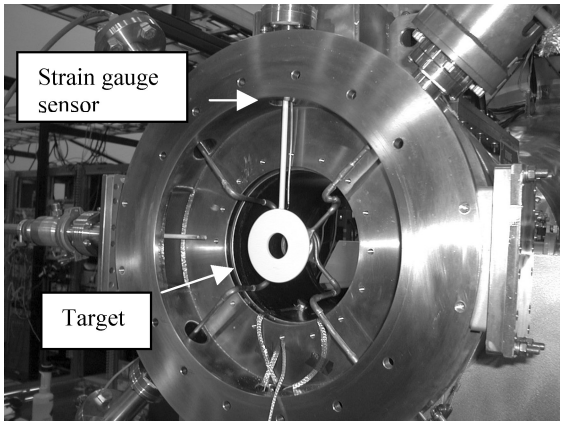

Fig. 7 Target with hole in center as front of test facility is removed.

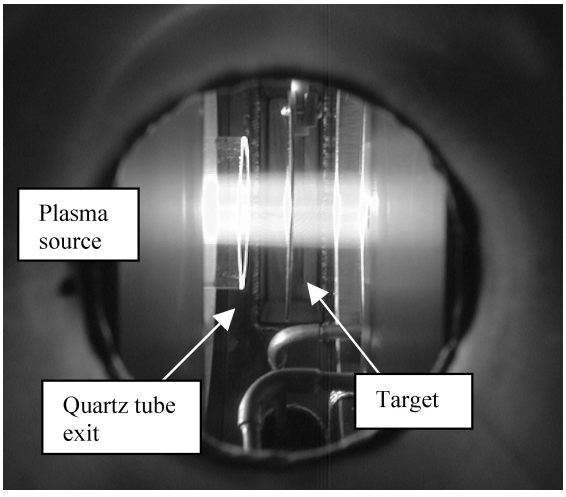

Fig. 8 Side view of target near quartz tube exit as plasma is flowing through center.

The following data are taken from a force sensor located upstream of the third magnet at the quartz tube exit. In the three-magnet configuration, as shown in Fig. 1, a target with a 3.2-cm-diam hole in the center was placed on the axis of the facility as shown in Fig. 7. A side view of the target plate with a hole in the center with the plasma flowing through the hole is shown in Fig. 8. The applied magnetic field is approximately 0.5 T and is directed perpendicular to the target at the location of the target shown in Fig. 8. The plasma is strongly magnetized with a plasma diameter of approximately 2.5 cm at this location and flows through the hole in the target. The neutrals are unaffected by the magnetic field and flow out of the 5-cm-diam quartz tube with velocity in the downstream direction.

The helicon antenna geometry was slightly different for this case, causing a different ionization fraction. Also, the flow rates are slightly different than for other data reported in this paper. However, the data do indicate that directed energy is given to the neutral particles exiting the plasma source. An assumption is made that the neutrals exiting the quartz tube are in a uniform beam and the beam is the diameter of the quartz tube. The fraction of neutrals exiting the quartz and penetrating the 3.2-cm hole in the momentum flux target is then 39% of the total neutrals. Given that the flow rate is 200 SCCM (9×10^{19} atoms/s) and the ion flow rate for the shot below is 10^{19} ions/s as determined by the langmuir probe, then 8×10^{19} atoms are exiting the quartz tube. Therefore, 61% of the exiting atoms are impacting the force sensor and applying the force measured below. This reasoning allows the determination of the average atom velocity in the downstream direction,

$$v = \frac{F}{\dot{m}} = \frac{0.0015}{(0.61)(8 \times 10^{19})(4 \times 1.67 \times 10^{-27})} = 4600 \text{ m/s} \quad (4)$$

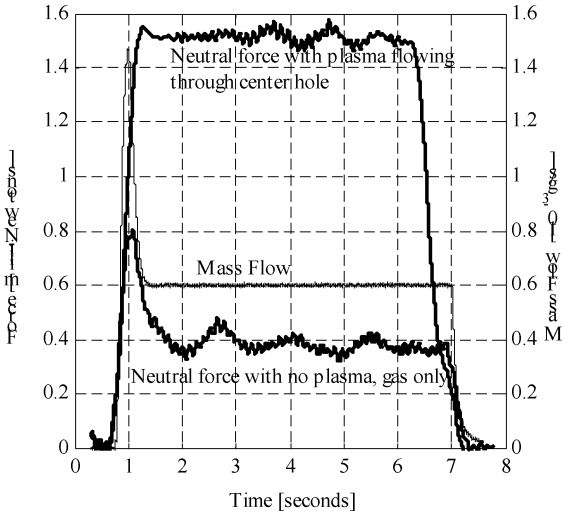

Fig. 9 Force of neutral particles with plasma on and off and normalized gas flow rate.

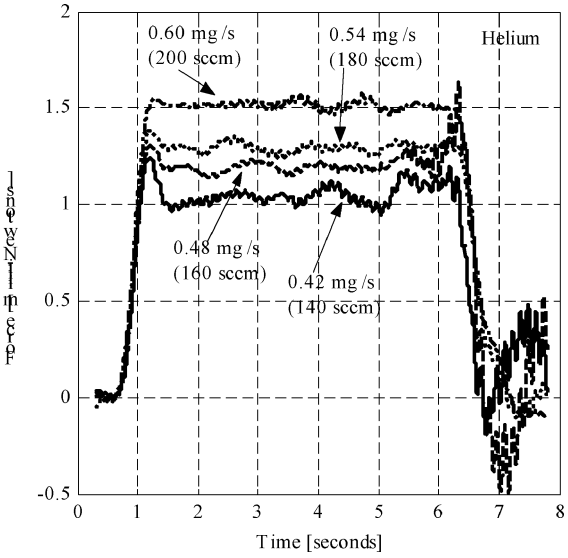

Fig. 10 Force from neutral particles energized by plasma.

where F, the force, is taken from Fig. 9. This value is approximately four times greater than the sound speed of ambient temperature helium. A possible mechanism for generating energized neutrals is charge exchange. Also, recent data indicate that the langmuir triple probe is indicating a slightly lower value for the electron density for helium discharges. With this correction, the ion rate is increased and the neutral rate is reduced, thereby allowing a larger velocity for the exiting neutrals. If so, the calculated ion rate will increase and the calculated value for the neutral velocity will increase. Figure 9 shows the effect of the plasma on the neutral momentum exiting the quartz tube. Figure 10 shows the effect of varying the gas flow on the neutral momentum. The langmuir triple probe correction is not quantified here but mentioned qualitatively to indicate that the reported neutral velocities are conservative.

IV. Heat Flux Measurement

The heat flux to a flat plate target was determined from the change in temperature of the target measured by type-K thermocouples connected to the rear of the target. The target was immersed in the plasma exhaust with the plasma impacting the front face. The target thickness or axial dimension was 2.4 or 3.2 mm while target diameters of 3.18, 5.1, 12.7, and 15.2 cm were tested. Heat flux data from the 12.7- and 15.2-cm-diam targets only are discussed in this paper. A cylindrical target was also used to recover the recombination energy without eliminating the flow momentum and will be discussed in a subsequent paper.

The heat flux on the target plate is due to kinetic and recombination energy. The heat flux due to kinetic energy is calculated from quantities determined by the electrostatic probes where these values are verified by the momentum flux measurement. The heat flux due to recombination is verified using the plasma parameters determined by the electrostatic probes. A metallic plate was placed in the plasma flow with the surface perpendicular to the flow direction, and four thermocouples, each at a different radial location, were attached to the rear of the plate to measure temperature rise of the plate. When Fourier's equation for heat conduction and an infinite slab geometry is used, a penetration depth δ and penetration time τ is given by (see Ref. 7)

$$\delta = 3.64\sqrt{\alpha t} \tag{5}$$

$$\tau = 0.0755(z^2/\alpha) \tag{6}$$

The penetration time of aluminum and titanium for a depth of 3.2 mm is determined to be 0.008 and 0.093 s, respectively. Only temperature data for the aluminum target will be discussed.

The axial thermal gradient was modeled using the one-dimensional differential equation for heat conduction in an isotropic material given by

$$\alpha \frac{\partial^2 q}{\partial z^2} = \frac{\partial q}{\partial t} \tag{7}$$

The solution for Eq. (7) is given by Carslaw and Jaeger for the temperature distribution of an infinite solid bounded by two planes.[8] Based on these results, the axial thermal gradient was taken to be negligible for these tests. The response of the thermocouple was different for each diameter target, as was expected. The larger diameter target was oversized to allow the entire plasma beam to be intercepted. However, this larger diameter target experienced a larger radial temperature gradient in the larger target as compared to the smaller target. Even with the larger target, a uniform temperature across the target was reached within a few seconds after the plasma was turned off, according to the predicted and measured values.

The smaller targets (3.18 and 5.1 cm diameter) allowed the entire target to be immersed in the plasma, and because the radial heat conduction was less, the target reached uniform temperature more quickly. Neglecting the axial thermal gradient and assuming axisymmetric heat flux allowed the radial thermal gradient to be modeled in one dimension. The one-dimensional radial heat conduction equation is given by

$$\rho c_p \frac{\partial T}{\partial t} + \frac{k}{r}\frac{\partial}{\partial r}\left(r\frac{\partial T}{\partial r}\right) = S(r,t) \tag{8}$$

where radiation losses are included in the source term $S(r, t)$. The solution to Eq. (8) is shown graphically (solid line) in Fig. 11a for the 15.2-cm-diam target along with the experimental data (dashed line) for the thermocouple located near the radial center of the target. There are nine plasma pulses lasting 5.5 s each with several seconds between the pulses. Targets with larger diameters than the plasma beam caused the center of the target to reach a higher temperature than the outer edges initially. The plasma beam diameter was approximately 9 cm. The heat from the center flowed out radially until the target reached an equilibrium temperature. The model was built to verify the heat flow and time required to reach thermal equilibrium, which was determined to be a few seconds. Figure 11b shows the temperature data for three radially distributed thermocouples attached to the backside of the 12.7-cm-diam target for a single plasma shot. Thermocouple 1 (TC 1) is located near the radial center of the target. TC 2 is located about 3 cm from radial center and TC 3 is located about 6 cm from radial center of the target. A fourth thermocouple was also attached to the rear of the target but a failure at the vacuum interface prevented data from some test; therefore, data for the fourth thermocouple are not shown. The heat flux onto the 12.7-cm-diam target for helium at 100 SCCM is 172 ± 1.5 W for

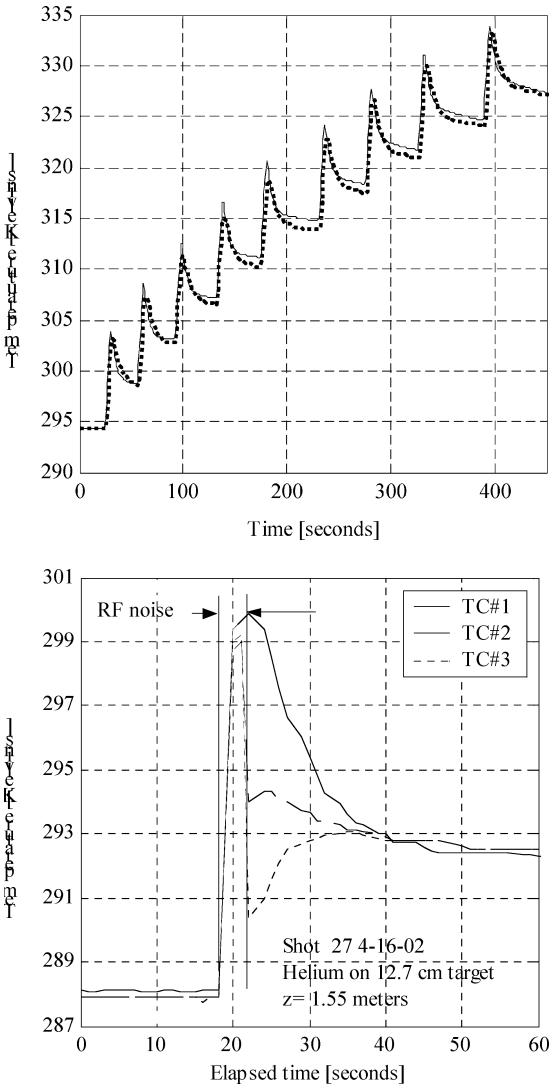

Fig. 11 Comparison of thermal model and experiment: a) experimental and thermal model data for 15.2-cm target and b) thermal data for one plasma shot.

six consecutive tests. The heat for argon at 25 SCCM was 51 ± 1 W and for 30 SCCM was 51 ± 2 W.

V. Analysis

The heat flux and momentum flux measurements could not be taken simultaneously. An attempt to mount the thermocouple on the momentum flux target plate caused uncertainties due to forces imparted on the target plate by the thermocouple. If the force on the momentum flux sensor from the thermocouple were constant during the plasma pulse, it could be subtracted as an offset. However, because the thermal expansion of the thermocouple wire as it is heated during the pulse may have induced a changing force, calibration of this changing force led to measuring the heat and momentum flux with separate instruments. The disadvantage of two separate instruments was that two separate plasma pulses were required, one for the momentum flux measurement and one for the heat flux measurement. This was acceptable because the electrostatic probes were used to verify that the plasma conditions remained similar for consecutive plasma shots.

The expected force on the plate may be calculated from known quantities and compared with the measured values. A langmuir triple probe and Mach probe are used to determine the electron temperature and density within a factor of two based on electrostatic probe theory.[9] A microwave interferometer was used to calibrate the triple probe to within a factor of 10% (Ref. 10). Two plasma parameters determined from electrostatic probes were the ion rate,

$$\Gamma_i = \int_0^R n_e(r) M(r) c_s(r)\, \mathrm{d}r = 1.3 \times 10^{19}/\mathrm{s} \tag{9}$$

and the average electron temperature,

$$k_B T_e = 5.3 \text{ eV} \tag{10}$$

where $M(r)$ is the Mach number, $c_s(r)$ is the ion acoustic speed, and $n_e(r)$ is the electron density. The volume flow rate of helium determined by the mks flow controller was 100 SCCM. Therefore, the rate of neutral particles exhausting during steady-state conditions is given by

$$\Gamma_n = \Gamma_{\text{total}} - \Gamma_i = 3.2 \times 10^{19}/\mathrm{s} \tag{11}$$

For argon at 30 SCCM, the neutral particle rate into the source is 1.3×10^{19}/s, and the neutral particle rate exiting is estimated to be 10^{19}/s because the ion rate for argon ions is approximately 0.3×10^{19}/s. The ions will be accelerated in the exhaust by the ambipolar electric field. The ambipolar electric field may be calculated by[10]

$$E = -(k_B T_e/|e|)(1/n_e)\nabla n_e \tag{12}$$

Equation (12) may be written as a change in electric potential between location 1 and location 2,

$$\Delta\phi_{21} = (k_B T_e/|e|)\, \ln(n_{e2}/n_{e1}) \tag{13}$$

Because the plasma is magnetized and will follow the magnetic lines of force in the region of measurement, the diverging magnetic field will cause an axial density gradient. The electron density, n_e, is used in Eqs. (12) and (13), but the plasma is quasi neutral so that the ion and electron densities are approximately equal. The number density in the following two equations refers to the plasma density that is equivalent to the electron and ion densities in the region of interest for this experiment. When conservation of magnetic flux ($\pi r^2 B$ = constant) is used, the change in density is related to the change in magnetic field by

$$n_2 = n_1(B_2/B_1) \tag{14}$$

The ions will then be accelerated as the magnetic field diverges. The acceleration of the ions will enhance the density gradient as determined by the continuity equation,

$$\frac{\partial n}{\partial t} + \nabla \cdot (n v) = 0 \tag{15}$$

The magnetic field reaches a peak value just axially downstream of the plasma source. The ions are assumed to reach approximately the ion acoustic speed at this axial location. The ion acoustic speed is given by

$$c_s \equiv \sqrt{k_B T_e/m_i} \tag{16}$$

The axial location of the peak magnetic field is just upstream of the exit of the quartz tube. The neutral pressure at this axial location is estimated to be a few millitorr providing a mean free path for ion-neutral charge exchange of only a few centimeters. The neutral pressure and density decrease just downstream of the quartz tube exit to near the background pressure in the vacuum chamber. At the mass flow rate used in this experiment, the mean free path for charge exchange is greater than 0.5 m in the exhaust region outside the quartz tube. Therefore, the fast moving neutrals are assumed to be created between the plasma source and the exit of the quartz tube. The charge exchange process involves a collision between an ion and a neutral. In this experiment, the ions are moving much faster than the ambient neutrals. The fast ion acquires an electron from the slow neutral thereby neutralizing the ion. The fast moving particle is now a neutral and is not affected by the electric or magnetic fields. The fast neutral has the velocity that the ion had before the collision.

The resulting ion has the velocity the neutral had before the collision and will be accelerated by the local electric field. The electrons are assumed isothermal throughout the exhaust because the mean free path for electron collisions with ions or neutrals is on the order of meters.

When the peak magnetic field is used as the reference point for determining the change in electric potential and the ions are assumed to be near the ion acoustic velocity at that location, the change in potential in volts from the peak magnetic field to $z = 1.55$ m is

$$\Delta\phi_{z=1.55} = 14.4 \tag{17}$$

and the change in potential in volts from the peak magnetic field to $z = 1.72$ m is

$$\Delta\phi_{z=1.72} = 21.7 \tag{18}$$

The force on the target plate from the ions may be determined by

$$F = \Gamma_i m_i v_i \tag{19}$$

This gives a force in newtons, for helium discharges, at $z = 1.55$ m of

$$F_{i,z=1.55} = 0.0025 \tag{20}$$

and at $z = 1.72$ m of

$$F_{i,z=1.72} = 0.0030 \tag{21}$$

where the change in force is due to the ambipolar acceleration of the ions.

As mentioned, the electrons are assumed isothermal throughout the exhaust so the force (in newtons) from the electron pressure is given by

$$F_e = An_e kT_e = 0.0011 \tag{22}$$

and is the same at both axial locations. The force from the neutrals is given by

$$F_n = \Gamma_n m_n v_n = 0.002 \tag{23}$$

where approximately 75% of the neutrals are assumed to impact the force sensor. This value is an estimate and can be accounted for by only slight radial diffusion of the neutrals. The force from the neutrals is assumed to be similar at both axial locations measured because the axial locations are only 0.17 m apart. Therefore, the total force on the plate at $z = 1.55$ m is calculated to be 0.0056 N and at $z = 1.72$ m is 0.0061 N, whereas the measured values are 0.0056 and 0.0063 N, respectively. These force values compare favorably to the momentum flux sensor data, which are taken to be steady state at 2 s into the plasma shot. A prepuff of propellant gas at a flow rate higher than the steady-state flow rate is used to initiate the plasma discharge. The plasma may reach steady state before 2 s, but the prepuff of propellant at the beginning of the plasma shot is observed to elevate the neutral pressure in the source region until approximately 2 s. The effect of the propellant prepuff is also observed on the momentum flux sensor.

If the force shown in Fig. 3 is assumed to be the thrust realized by the device, then the specific impulse for the helicon source is given by

$$I_{\rm sp} = \frac{F}{\dot{m}g} = \frac{0.006\,\text{N}}{(3\times10^{-7}\ \text{kg/s})(9.8\ \text{m/s}^2)} = 2000\ \text{s} \tag{24}$$

This value of specific impulse comprises the combined charged and neutral particle jets. Accounting for reflection of the particles will reduce the measured momentum by 20% (Ref. 11). The force values shown earlier did not account for the 20% reduction due to momentum reflection.

The change in temperature of the target was used to calculate the heat flux or absorbed power using

$$q(t) = mc_p \frac{\mathrm{d}T}{\mathrm{d}t} + \alpha(T - T_s) + \varepsilon\sigma\left(T_p^4 - T_{\rm ch}^4\right)A_r \tag{25}$$

The initial temperature used in Eq. (25) was taken at the beginning of the plasma pulse, whereas the final temperature was taken after the plasma pulse when the target reached thermal equilibrium (about 15 s). The target size and mass were 12.7 cm and 0.086 kg for the measurements analyzed in this experiment. The heat flow to the target for six consecutive plasma shots using Eq. (25) and measured values of temperature was determined to be 172 ± 2.2 W.

The heat to the surface may be calculated using

$$q_{\rm plasma} = \Gamma_i\left[\left(\tfrac{1}{2}m_i v_i^2 - |e|\phi_f\right)(1 - R_{iE}) + 2kT_e/(1 - \delta_e) + E_{\rm rec}\right] \tag{26}$$

where the ion temperature has been neglected and the presheath acceleration has been neglected because the ion speed is greater than the ion acoustic speed before reaching the sheath.[11] A presheath electric field exists when plasma is flowing at speeds lower than the ion acoustic speed and will accelerate the ions to the ion acoustic speed required by the Bohm criteria at the plasma–sheath boundary (see Ref. 12).

When Eq. (26) and the parameters used to calculate the force values in Eqs. (20), (22), and (23) are used, the expected heat flow (in watts) to the plate at $z = 1.55$ m is

$$q_{\rm net} = q_{\rm plasma} + q_n = 169 \tag{27}$$

where the neutral contribution to the heat flow q_n is 9.2 W and the heat (in watts) from the plasma recombination at the surface is

$$q_{\rm rec} = \Gamma_i E_{\rm rec} = 51 \tag{28}$$

and was included in Eq. (27). The energy released by each ion–electron pair on recombination for helium is 24.6 eV and for argon is 15.7 eV. As observed, the recombination energy accounts for approximately 30% of the energy in the plasma exhaust at the axial location of this experiment.

Repeating the same analysis using the argon data, the average $I_{\rm sp}$ is found to be

$$I_{\rm sp} = \frac{0.006\,\text{N}}{(8.9\times10^{-7}\ \text{kg})(9.81\ \text{m/s})} = 685\ \text{s} \tag{29}$$

This is equivalent to an average directed energy of the argon ions and neutrals of 9.4 eV. The ions are likely more energetic than this. Although this is less than desired, recent modifications to the test facility have given indications that the ionization fraction is approaching 100% (Ref. 13).

VI. Discussion

As shown in Fig. 3, the steady-state force at the axial location corresponding to a magnetic field of 0.026 T, is approximately 6.4 mN. At 17 cm nearer the magnetic choke where the magnetic field has a value of 0.083 T, the force is 5.5 mN. If neither plasma source nor sink exists between the two axial locations and the force targets are larger than plasma column diameter, the increase in force is likely due to acceleration of the flow. The ionization fraction was determined to be approximately 22%. The force measured by the force sensor is composed of both charged and neutral particle jets. The charged particles are confined to the magnetic field lines and will impact the force target. However, the neutral particles will likely diffuse with only some fraction of the neutrals exiting the plasma source impacting the force target plate. The exact value of the force due to neutrals was yet to be determined. However, data acquired using a force sensor with an aperture in the center of the target, allowing the confined plasma to pass but intercepting the neutrals outside the plasma column, indicate that kinetic energy is given to the neutrals in the axial direction. A conservative estimate is that the entire flow impacts the target. The average particle velocity neutral and ion, may then be determined by

$$v = F_{\rm th}/\dot{m} \tag{30}$$

This yields an average velocity of 18.5 km/s upstream and 21.5 km/s at a location 17 cm downstream.

An ionization fraction of 100% is desired when using the helicon as a plasma source only. However, allowing some fraction of the flow to be neutral particles such that an optimized number of charge exchange and elastic collisions occurs between the neutral and ions may increase the thrust without reducing the efficiency. The increased thrust will be at the expense of the I_{sp}. As discovered in this investigation, ion momentum is given to the neutral particles through collisions. Without recovering the ionization energy, the thrust may be increased at constant power. If this is accomplished, the energy efficiency will not decrease as the specific impulse is lowered. For example, consider an ion accelerated by the ambipolar electric field to a kinetic energy of E_i. The momentum of the ion is given by

$$P_1 = m_i v_i = m_i \sqrt{2E_i/m_i} = \sqrt{2m_i E_i} \tag{31}$$

Next, consider the charge exchange collision of an ion (different ion) with a neutral at the axial location where the ion has only been accelerated to energy of $\frac{1}{2}E_i$. After the charge exchange collision, the neutral will have kinetic energy $\frac{1}{2}E_i$ and the ion will have very little kinetic energy. The ion is then accelerated by the ambipolar electric field to $\frac{1}{2}E_i$. The combined energy of the neutral after charge exchange and the ion after being accelerated through the remaining ambipolar field will be E_i. Therefore, the energy is the same as that of the single ion in Eq. (31). However, the momentum of the two particles will be

$$p_2 = m_1 v_1 + m_2 v_2 = 2mv = 2\sqrt{2m\tfrac{1}{2}E_i} = 2\sqrt{mE_i} \tag{32}$$

where the subscripts 1 and 2 denote neutral particle and ion, respectively. The mass of the neutral particle and the mass of the ion were assumed the same in Eqs. (31) and (32). Therefore, the momentum in the flow is increased by

$$P_2/P_1 = \sqrt{2} \tag{33}$$

The thrust realized by the thruster will also be increased by this amount but at the expense of specific impulse. If the neutral density can be controlled to allow each ion to only experience at most a few charge exchange collisions at the correct axial location, the thrust can be increased at constant energy input thereby improving the energy cost per particle in the exhaust because many of the ejected particles will be neutrals.

VII. Conclusions

The data presented show that the momentum and energy flow determined from the experiment agrees well with calculated values, providing a reasonable estimate of particle and power balance within the exhaust region of the experiment. The expected thrust from the device could not be accurately determined from these momentum flux measurements because the sensor was not located at the optimum axial location and the device was configured to provide maximum thrust. The VX-10 test facility was configured for plasma source optimization to provide target plasma for the ion booster stage. However, this diagnostic technique was demonstrated to provide an estimate of the momentum and energy flux in the plasma flow. These flux values provide information about the flowing plasma and can be used to determine relative changes, and perhaps absolute changes, in expected thrust generated by plasma propulsion devices. Several sizes of flat targets were tested at various test conditions but only a small subset was discussed in this paper. Experiments were conducted to recover the recombination energy and still permit the momentum to be partially preserved by exhausting only neutral particles have been successfully performed. These results will be presented in a subsequent paper.

Investigation of momentum flux using heavy gases should be accomplished to determine the feasibility of using the heavy gases to reduce the frozen losses when operating in the high thrust/low specific impulse operating regime. Injection of a heavy gas, argon, into deuterium and helium was investigated and will be discussed in a subsequent submission. Further investigation of combining different species of gas may provide a means of varying the specific impulse and thrust.

References

[1]Arefiev, A. V., and Breizman, B. N., "MHD Scenario of Plasma Detachment in a Magnetic Nozzle," *Physics of Plasmas*, Vol. 12, Article 043504, April 2004.

[2]Hagstrum, H. D., "Theory of Auger Ejection of Electrons from Metals by Ions," *Physical Review*, Vol. 96, No. 2, 1954, pp. 336–365.

[3]Chang-Diaz, F. R., "The VASIMR Engine: Concept Development, Recent Accomplishments and Future Plans," *Open Systems, Transactions of Fusion Science and Technology*, Vol. 43, No. 1, 2002.

[4]Squire, J. P., Chang-Diaz, F. R., Jacobson, V. T., McCaskill, G. E., Bengtson, R. D., and Goulding, R. H., "Helicon Plasma Injector and Ion Cyclotron Acceleration Development in the VASIMR Experiment," *36th Joint Propulsion Conference*, AIAA, Reston, VA, 2000.

[5]Chavers, D. G., and Chang-Diaz, F. R., "Momentum Flux Measuring Instrument for Neutral and Charged Particle Flows," *Review of Scientific Instruments*, Vol. 73, No. 10, 2002, pp. 3500–3507.

[6]Chavers, D. G., "Recombination Processes in a Flowing Magnetized Plasma: Application to Ionization Energy Recovery in the Variable Specific Impulse Magnetoplasma Rocket (VASIMR)," *Physics*, The Univ. of Alabama in Huntsville, Huntsville, Alabama, 2003, p. 190.

[7]White, F. M., *Heat Transfer*, Addison–Wesley, Reading, MA, 1984, p. 169.

[8]Carslaw, H. S., and Jaeger, J. C., *Conduction of Heat in Solids*, Oxford Univ. Press, London, 1959, Chap. 3.

[9]Bering, E. A., Bruhardt, M., Chang-Diaz, F. R., Squire, J. P., Jacobson, V., Bengtson, R. D., Gibson, J. N., and Glover, T. W., "Experimental Studies of the Exhaust Plasma of the VASIMR Engine," AIAA Paper 2002-345, Jan. 2002.

[10]Hutchinson, I. H., Principles of Plasma Diagnostics, Cambridge Univ. Press, New York, 2002, Chap. 4.

[11]Stangeby, P. C., *The Plasma Boundary of Magnetic Fusion Devices*, Inst. of Physics, Bristol, England, U.K., 2000, Chap. 3.

[12]Chen, F. C., *Introduction to Plasma Physics and Controlled Fusion*, Plenum, New York, 1984, Chap. 8.

[13]Squire, J. P., Chang-Diaz, F. R., Jacobson, V. T., Glover, T. W., Baity, F. W., Goulding, R. H., Bengtson, R., Bering III, E. A., and Stokke, K. A., "Experimental Research Progress Toward The VASIMR Engine," *Proceedings of the 28th International Electric Propulsion Conference*, Centre National d'Etudes Spatiales, Toulouse, France, 2003.